

Cryogenic Memory Technologies

Shamiul Alam¹, Md Shafayat Hossain², Srivatsa Rangachar Srinivasa³, and Ahmedullah Aziz^{1*}

¹Dept. of Electrical Eng. & Computer Sci., University of Tennessee, Knoxville, TN, 37996, USA

²Dept. of Physics, Princeton University, Princeton, NJ, 08544, USA

³Intel Labs, Hillsboro, OR, 97124, USA

*Corresponding Author's Email: aziz@utk.edu

Abstract—The surging interest in quantum computing, space electronics, and superconducting circuits has led to new, recent developments in cryogenic data storage technology. Quantum computers and superconducting single flux quantum (SFQ) electronics promise the ability to solve the challenges (such as currently unsolvable problems and speed-power issues) faced by their conventional and semiconductor counterparts, respectively. But, one of the major bottlenecks for implementing scalable quantum computers and practical SFQ circuits is to find a suitable and compatible cryogenic memory that can operate at 4 Kelvin (or lower) temperatures. Cryogenic memory is also critically important in space-based applications. Different memory technologies, such as non-superconducting memories like charge-based and resistance-based memories, Josephson junction-based superconducting memories, and hybrid (utilizing both non-superconducting and superconducting technologies) memories, are being explored to find a suitable storage system for the promising cryogenic applications. Here we review the variants of cryogenic memory technologies and scrutinize the challenges associated with these technologies and discuss future research prospects.

Index Terms— Cryogenics, Cryogenic Memory, Quantum Computer, SFQ Circuits, Superconducting Electronics.

1. Introduction

Silicon-based complementary metal-oxide-semiconductor (CMOS) technology now allows us to accommodate more than billion transistors on a chip (for example, Cerebras Wafer Scale Engine 2 with 2.6 Trillion transistors ¹). However, this aggressive scaling comes with a price- an exorbitant power dissipation reaching the physical limit. For example, in 2018, about 205 TWh of electricity was consumed by the US data centers ². To circumvent this issue, numerous ‘beyond-CMOS’ technologies, such as superconducting single flux quantum (SFQ) electronics, are being explored. Superconductive devices [e.g., Josephson junctions (JJ) and superconducting quantum interference device (SQUID)] based SFQ circuits and systems are generally faster and more energy-efficient than the CMOS devices ³, thanks to the dissipation-less current flow in superconductors. Ultrafast and energy-efficient superconducting SFQ circuits, coupled with lossless and low dispersion interconnects, have significantly improved performance in different applications such as digital radio frequency receivers ^{4,5}, high-end computing ⁶, and so on. However, the lack of fast, low-power, high-density cryogenic memory compatible with the performance of SFQ circuits is one of the significant challenges for implementing practical and reliable SFQ systems.

Going beyond the conventional computing paradigm, the importance of cryogenic memory is felt in quantum computers as well. Among the different platforms for quantum computations, superconducting qubits have attracted immense attention thanks to their non-dissipative and strongly non-linear behavior ⁷⁻¹⁶. Quantum computers promise to solve commercially and scientifically important problems that the current classical computers can hardly handle in a realistic timeframe. For instance, accurate simulation of large molecules for the development of new drugs and eco-friendly manufacturing processes now require unrealistic time due to exponential scaling of the complexity in classical computers. However, these simulations can be performed with a quantum computer in polynomial time ¹⁷. Moreover, quantum computers can significantly accelerate number theory, algebraic, and optimization problems ¹⁸. However, the lack of a suitable cryogenic memory is a major challenge in implementing a scalable quantum computer.

Space-based application is another major field that can highly benefit from the utilization of cryogenic devices. JJ and SQUID-based cryogenic equipment have been used in several spacecrafts in the last few decades ¹⁹. The utilization of cryogenic devices has enabled the spacecrafts to work with the electromagnetic radiation emitted by celestial objects over a wavelength range that is difficult to work with from the ground. The utilization of cryogenic electronics is

expected to improve efficiency and reliability and simplify the design of the space systems, thanks to the improvement in electrical, electronic, and thermal properties of materials at cryogenic temperatures^{20,21}.

In this review, we will discuss state-of-the-art cryogenic memory technologies. We organize our discussion as the following: *Section 2* delineates the benefits of using cryogenic memory in quantum computers and cryogenic electronics, as well as the required characteristics of a cryogenic memory for these applications. Next, in *Section 3*, we review different cryogenic memories, namely cryogenic non-superconducting memories [e.g., charge-based memories and resistance-based memories], superconducting memories [such as superconductor-insulator-superconductor (SIS) JJ-based, magnetic JJ-based, and superconducting memristor-based approaches], and hybrid memories (utilizes both superconducting and non-superconducting technologies). In *Section 4*, we present a comparative study among these cryogenic memories. Here we outline the major challenges faced by different cryogenic memories and conclude with the research prospects on developing a suitable cryogenic memory.

2. Why Cryogenic Memory?

Cryogenic memories are proven to be critical in quantum technologies. A typical quantum computer has three major components: quantum substrate (qubits), a control processor, and a memory block⁸ [see Fig. 1(a) which illustrates the organization of a scalable quantum computer proposed in Ref. ²²]. In quantum computing, qubit is the basic unit of quantum information realized with a two-state device. Qubits are very sensitive to noise and hence, to protect the qubit states from thermal noise, qubits are placed at a few milli-Kelvin temperatures^{10–15}. In the current lab size quantum computers, a conventional computer at room temperature (300 K) is used as the control processor. Long control cables are required to connect the qubits and the control processor. Although this architecture works fine for a small number of qubits, it cannot be scaled to a few hundreds of qubits because it would require a large number of wires to establish a connection between the room-temperature control processor and the qubits at cryogenic temperature⁸. Note, the quantum computer needs to be scaled up to thousands of qubits to utilize its full potential. For example, to run Shor's algorithm for prime factorization¹⁸, which is a textbook quantum algorithm, on a 1024-bit number in a quantum computer, two quantum registers (one with 2048 qubits and another with 1024 qubits) are required. To circumvent this scaling issue, the control processor should be placed at a temperature very close to that of the qubits using the superconducting interconnects²³. Also, the use of superconducting interconnects instead of metal wires would also be beneficial because of the dissipationless nature and ability of high density of the superconducting interconnects. But, to use superconducting interconnects, the control processor needs to be placed at 4 K or below. It places yet another restriction in the type of memory that can be used in conjunction with quantum computers: room temperature memories cannot be used because the interconnects between the room-temperature memory and the cryogenic control processor would have a significant thermal leakage. This leakage stems from the huge temperature difference (about 300 K) between the room and cryogenic temperature and contributes to thermal noise that is large enough to destroy the quantum states of the noise-sensitive qubits⁸. An obvious way-around is to use a cryogenic 4 K memory, which is compatible with the superconducting control processor.

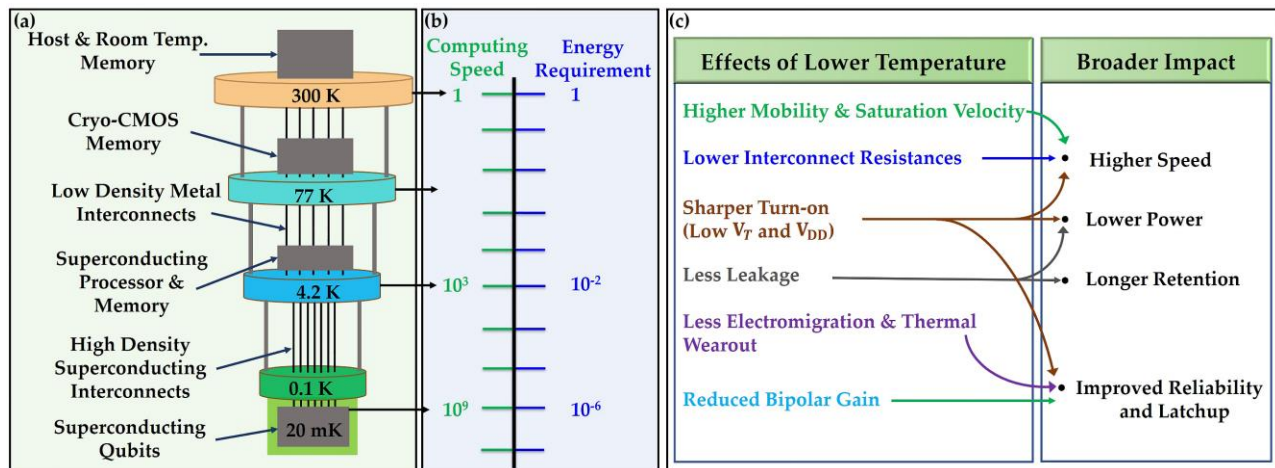


Fig. 1: (a) Proposed organization of a superconducting quantum computer²². Control processor operating at 4 K provides instructions to the qubits operating at 20 mK. Possible memory locations are 4 K, 77 K and 300 K. (b) Significant increase in speed and decrease in energy with the lowering of operating temperature. Speed and energy have been normalized by the values at 300 K. (c) Effects of cryogenic temperature on the traditional CMOS devices. Lower temperature improves the speed, power requirement, retention time and reliability of the CMOS memories²⁹.

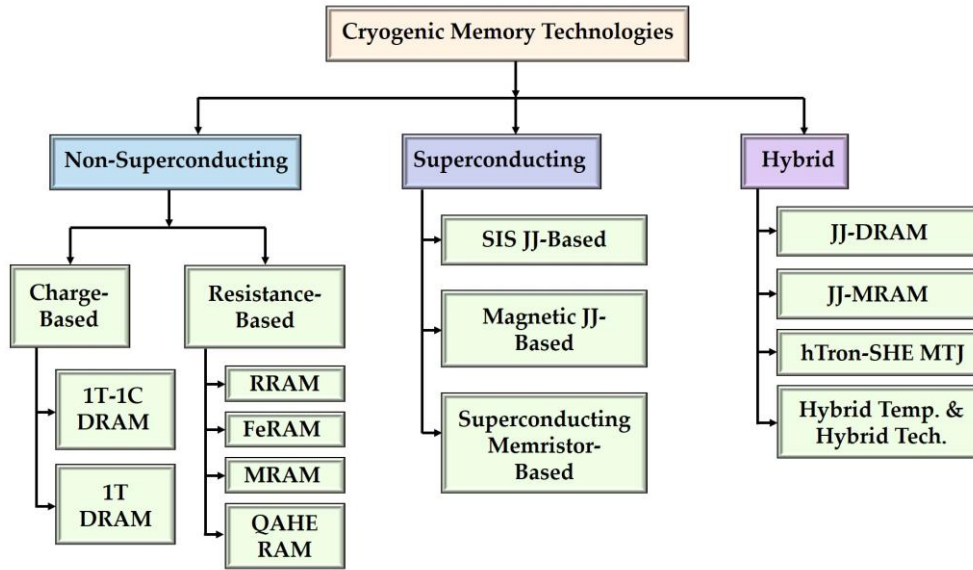


Fig. 2: Taxonomy of state-of-the-art cryogenic memory technologies.

Another key requirement for the storage device of a quantum computer is its high storage capacity. The state-of-the-art quantum algorithms require a large number of arbitrary rotations which eventually necessitate a large program memory⁸. Furthermore, to preserve the data integrity of the qubit states, the qubits undergo continuous error correction schemes^{8,11}; it requires extensive memory and bandwidth.

Although 4 K memories promise better scalability of the quantum computer and very low thermal leakage, researchers have explored the option of placing memories at a temperature higher than the processor temperature because the cost for cooling the memory systems down to 4 K is ≈ 200 times higher compared to the room temperature memory^{10,22}. Albeit there is little thermal leakage, memories placed at a higher temperature (such as 77 K) than 4 K also provide larger capacity along with the lower cost¹⁰. Figure 1(a) highlights all these possible memory placements in a superconducting quantum computer.

Cryogenic memories are also crucial for superconducting SFQ electronics. To solve the speed and power issues faced by CMOS technology²⁴, superconducting electronics is an attractive solution, thanks to the faster and more energy-efficient operations offered by superconducting devices such as JJs and SQUIDs. Figure 1(b) depicts the significant reduction in power requirement and increase in speed with the lowering of operating temperature. However, according to the National Security Agency, the lack of a scalable, compatible, and 4 K memory system is one of the major challenges that has limited the superconducting electronics only in niche applications⁶. The reason for the requirement of a 4 K memory in SFQ technologies is the lower power and latency afforded by the physical proximity^{6,25}.

In the next section, we list the frontrunners in the cryogenic memory technologies and discuss how they perform compared to the requirements mentioned above in this section.

3. Overview of State-of-the-art Cryogenic Memories

Here, we highlight the state-of-the-art cryogenic memory architectures, such as charge and resistance-based non-superconducting memories, JJ and SQUID-based superconducting memories, and hybrid memories implemented using both non-superconducting and superconducting technologies. For ease of discussion, we first categorize the state-of-the-art cryogenic memories as shown in Fig. 2.

3.A. Cryogenic Non-Superconducting Memories

Our discussion starts with the non-superconducting memories for cryogenic applications. These memory devices are prime candidates for cryogenic memory, thanks to their technological maturity and their ability to offer high capacity. Remarkably, a CMOS control processor for quantum computers that can operate at 4 K has recently been reported¹¹; it permits a close integration between superconducting qubits and CMOS control processors. Then the remaining

question is whether or not the conventional non-superconducting memories work in cryogenic temperatures.

Yoshikawa *et al.*²⁶ suggested that CMOS devices and circuits operate better at 4 K than the room temperature for several sub-micron CMOS processes. The speed improves by 40% to 50% and the power dissipation reduces by 30% (depending on the circuit operation) for digital circuits at 4 K compared to the room temperature²⁶. However, operating at 4 K temperature poses two important challenges. First, 4 K-temperature devices can sustain only at low powers. Second, as discussed in section 2, 4 K operation entails significantly higher costs. Operating at a slightly higher temperature can offer an optimized solution to these challenges.

As shown in Fig. 1(a), 20 mK, 4 K, 77 K, and 120 K are the temperature levels of a typical cryogenic (dilution) refrigerator⁸. A natural choice is to run the CMOS memory operations at 77/120 K. These temperatures still reduce the leakage current substantially and improve the carrier mobility²⁷, leading to an enhancement in the driving capability of access transistors, and the overall memory operation. Importantly, these temperatures are within the ideal operating temperature range for the CMOS devices. Figure 1(c) shows the improvement in different performance metrics of CMOS devices with the lowering of temperature. In turn, placing a memory at a slightly higher temperature than 4 K cuts down the cost substantially. While this scheme may work for smaller quantum computers, it will most certainly limit the scaling of the quantum computer due to the large number of connections between the 77/120 K memory and the 4 K control processor and the resulting thermal loss. Moreover, some emerging memories have been reported to show successful operation at 4 K temperature. So, for the non-superconducting memories, the main challenge is their requirement of higher power and lower speed compared to the control processor at 4 K.

To facilitate our discussion, we classify the non-superconducting memories into two major categories: (i) charge-based and (ii) resistance-based. In the following subsections, we will introduce different members of these two families.

3.A.1. Charge-based Memories

First, we discuss the different variants of CMOS dynamic random-access memory (DRAM). In the charge-based memories, data is stored in a small capacitor. The capacitor can either be charged or discharged which provides the two memory states ('0' and '1') in the cell. There are two main categories of DRAMs: DRAM with capacitor [mostly known as 1-Transistor 1-Capacitor (1T1C) DRAMs] and capacitorless DRAM [known as 1-Transistor (1T) DRAMs].

3.A.1.1. 1-Transistor 1-Capacitor (1T1C) DRAMs

1T1C DRAMs [see Fig. 3 (a)] are one of the strong candidates for cryogenic memory because of their technical maturity, the ability to offer very high capacity, and expected performance improvements at low temperatures due to the reduced junction leakage of cell transistors^{8,10,11}. Low-operating temperature also reduces the required refresh power and switching energy¹⁰. In the late 1980s, IBM first demonstrated low temperature (85 K) 512 Kbit^{27,28} and 4 Mb²⁹ DRAMs with a significant improvement in speed and retention time compared to the DRAMs at room temperature. High carrier mobility at lower temperatures led to significant improvement in the performance of these DRAMs at cryogenic temperatures.

Fast forward to 2017, Tannu *et al.*⁸ developed an experimental setup to characterize the high-density DRAMs for quantum computing applications. They examined DRAM chips over a temperature range of 80 K to 160 K. By testing 55 DIMMS (with 750 DRAM chips) from six different vendors, Tannu *et al.*⁸ concluded that a significant number of the chips continues to work perfectly at cryogenic temperatures. Also, the error patterns (mainly transient error and permanent error) observed at cryogenic temperatures are uncorrelated errors that can be solved with conventional correction schemes like forward error correction Chipkill and sparing⁸.

Consequently, Ware *et al.* investigated the feasibility of using 77 K DRAMs in quantum computing systems¹⁰ and reported that DRAMs work well at 77 K without any functional errors. However, the major challenge for 77 K DRAMs is the requirement of a link interface with low thermal conductivity (a flexible cable³⁰) to connect to the control processor placed at 4 K.

Another version of the CMOS DRAM is the 3-transistor (3T) DRAM cell [see Fig. 3(b) for the schematic], where two additional transistors are used for the readout purpose. The advantage of 3T DRAM cell over 1T1C DRAM is that 3T DRAM requires simpler peripheral circuitry for write and readout purposes³¹. Yoshikawa *et al.*²⁶ characterized 3T DRAM cells at 4 K temperature for their hybrid Josephson-CMOS memory implementation (discussed in Section 3.C).

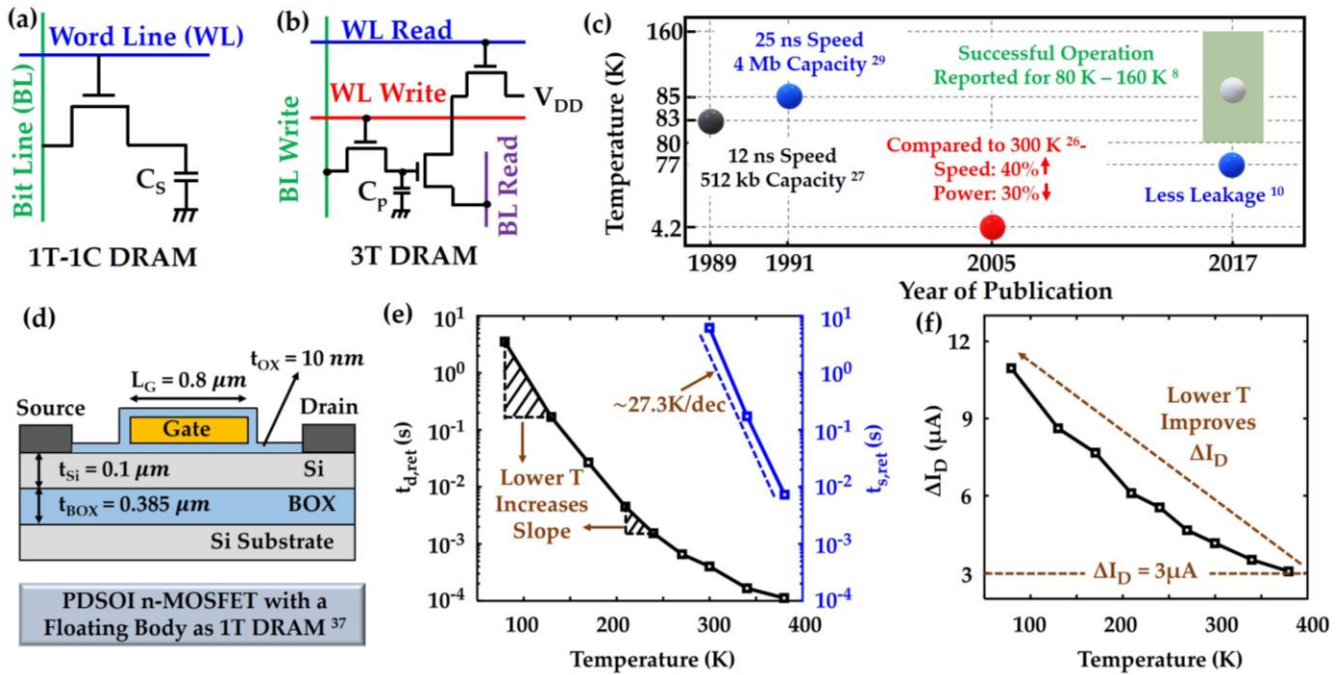


Fig. 3: Schematics of (a) 1T1C DRAM, (b) 3T DRAM cells. In 1T1C DRAM, the capacitor C_S stores the data whereas in 3T DRAM, the parasitic capacitance stores the data. (c) Major attempts on cryogenic DRAMs over the years. The reported effects of cryogenic temperature on different performance metrics are also mentioned. (d) Schematic of a PDSOI n-MOSFET with floating body³⁷ that can act as a capacitorless DRAM. Temperature dependence of (e) static retention time, $t_{s,ret}$ and dynamic retention time, $t_{d,ret}$, and (f) current sensing margin, ΔI_D . $t_{s,ret}$ and $t_{d,ret}$ sharply increase, and ΔI_D improves at lower temperatures.

This work reported a 40% improvement in speed and a 30% reduction in power consumption at 4 K compared to 300 K.

We summarize the attempts on cryogenic DRAMs (with capacitor) in Fig. 3(c) highlighting the operating temperature and significant performance improvements reported at cryogenic temperatures compared to their room temperature operations.

3.A.1.2. Capacitorless 1-Transistor (1T) DRAMs

Thanks to the highly scalable structure compared to the 1T1C DRAM cells^{32–36}, capacitorless single transistor DRAM (1T-DRAM) devices have been explored to construct scalable memory systems. Going towards low temperatures improves the performance of the 1T DRAM cells by reducing the generation and recombination of carriers [14], a major retention failure mechanism of the 1T DRAM cells. Furthermore, an important feature of these memories is their compliance with the high density, high capacity memory applications; this is an important requirement for quantum computer systems. These clear advantages make this memory type a strong candidate for cryogenic memory.

Very recently, a cryogenic 1T-DRAM cell (with operation over a temperature range of 380 K to 80 K) has been implemented via a partially depleted silicon-on-insulator (PDSOI) n-MOSFET with a floating body³⁷; see Fig. 3(d) for the schematic illustration. Four memory operations (write ‘0’, write ‘1’, hold, and read) have been implemented by choosing suitable bias conditions for the gate and drain of the transistor. As mentioned in the previous paragraph, one of the major drawbacks of the capacitorless DRAM cells is the retention failure which is improved significantly here at low temperatures. Figure 3(e) shows the temperature dependence of the static retention time, $t_{s,ret}$ (during hold operation) and dynamic retention time, $t_{d,ret}$ (during read operation) reported in this work which shows that both the retention times improve significantly at lower temperatures. A significant improvement in the current sensing margin (ΔI_D) has also been reported at lower temperatures compared to that at 300 K [Fig. 3(f)].

3.A.2. Resistance-based Memories

Compared to the charge-based memories, resistance-based memories offer better scalability, faster speed, and lower power consumption³⁸. Moreover, resistance-based memories offer non-volatility. In these memory cells, two resistance states [known as high resistance state (HRS) and low resistance state (LRS)] define the two memory states (‘0’ and

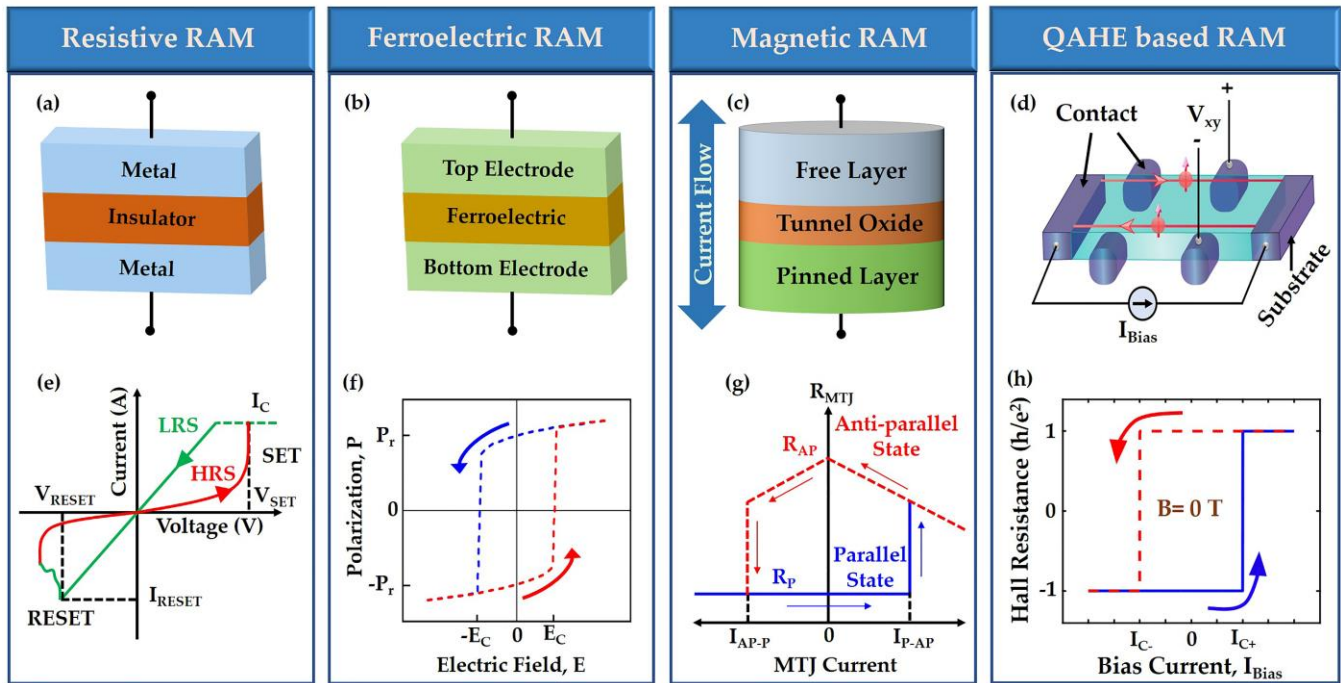


Fig. 4: Schematic structures of (a) ReRAM, (b) FeRAM, (c) MRAM, and (d) QAHE-based RAM. Signature hysteresis in (e) the I - V characteristics of ReRAM, (f) in the P - E characteristics of FeRAM, (g) in the MTJ resistance vs MTJ current characteristics of MRAM, and (h) in the Hall resistance vs bias current characteristics of QAHE-based RAM. The characteristics shown in (e)-(h) demonstrate the two resistance states (HRS and LRS).

‘1’, respectively). Resistive RAM (ReRAM), ferroelectric RAM (FeRAM), magnetic RAM (MRAM), quantum anomalous Hall effect (QAHE) based RAM, and phase-change RAM (PCRAM) are the members of the resistance-based memory family. Figure 4 shows the schematic structures of all the members of this family as well as their signature hysteretic characteristics containing the two resistance states required for the memory operations.

3.A.2.1. Resistive Memories

Resistive random-access memory (ReRAM), i.e., metal-insulator-metal (MIM) sandwiched between two electrodes [see Fig. 4(a)], is another strong candidate for cryogenic memory thanks to its low power operations, excellent scalability, high reliability, and simple manufacturing processes^{39,40}. The I - V characteristics of these devices show a hysteretic response where two distinct resistance states (HRS and LRS) are observed [see the illustration in Fig. 4(e)]. Resistive switching has been observed in numerous material systems, such as binary transition-metal oxides (e.g., NiO⁴¹, TiO₂⁴², and HfO₂⁴³), perovskite-type oxides⁴⁴, silicon oxides⁴⁵, and even single-molecule systems⁴⁶. Among these HfO₂ based ReRAMs shows the most promise as a cryogenic memory⁴⁷⁻⁵¹.

Back in 2014, Ahn *et al.* analyzed the I - V characteristics of Pt/Al₂O₃/HfO_x/Er/Pt ReRAM device over the temperature range of 40 K to 350 K⁴⁸ and it has been reported that the lower the temperature becomes, the more resistive the device becomes in both LRS and HRS. Intriguingly, the device in LRS has a greater dependence on temperature than the one in HRS. Later, Shang *et al.*⁴⁹ demonstrated the memory operation of ITO (indium-tin-oxide)/HfO_x/ITO MIM structure with a large R_{OFF}/R_{ON} ratio, excellent endurance (5×10^7 cycles), extrapolated retention ability (over 10^6 s) and a wide working temperature range of 10 K to 490 K. This work showed that the ON-state resistance (R_{ON}) decreases and the OFF-state resistance (R_{OFF}) increases with the lowering of the temperature and therefore, the R_{OFF}/R_{ON} ratio increases at lower temperatures, but with the cost of larger set/reset voltages. Not so long after, in 2015, Fang *et al.*⁵⁰ demonstrated proper resistive switching for Pt/HfO_x/TiN devices at ultra-low temperatures (4 K and 77 K). Here also the resistances in both LRS and HRS increase with the lowering of the temperature. Bolonkowski *et al.* improved this structure and found that TiN/Ti/HfO₂/TiN devices can operate between 4 K to 300 K temperatures. In contrast to the previous two efforts, here the resistive switching exhibited no significant change at lower temperatures⁵¹. Considering the demonstration of proper switching between LRS and HRS in HfO_x based ReRAM devices at ultra-low and low temperatures, these ReRAM devices can also be explored as a potential cryogenic memory.

3.A.2.2. Ferroelectric Memories

Ferroelectric memory is a promising non-volatile memory. The construction of FeRAMs is similar to ReRAMs, but the only difference is that a ferroelectric layer is used instead of a dielectric/insulating layer [see Fig. 4(b)], which creates the non-volatility in FeRAMs. The hysteretic polarization (P) vs electric field (E) curve, the signature of the ferroelectric memories, is shown in Fig. 4(f). The advantages of FeRAMs include low power consumption, fast speed, large endurance (about 10^{10} to 10^{14} cycles), and retention time of more than 10 years⁵².

Ferroelectric field-effect transistor (FeFET), a three-terminal ferroelectric device, is the most explored ferroelectric memory. FeFETs also provide nanosecond program/erase time, high scalability, low voltages, and dense analog states⁵³⁻⁵⁶. Therefore, the properties of the ferroelectric materials (an integral part of FeFET) have been extensively studied over the last few decades down to the milli-Kelvin temperature range⁵⁷⁻⁶⁰. Very recently, the cryogenic characteristics of an n-type FeFET, which includes a silicon doped hafnium oxide (Si: HfO₂) as a ferroelectric layer, have been studied up to 6.9 K temperature⁶⁰. This work reports that the decrease in temperature causes an increase in the memory window with the cost of an increase in the program/erase voltage. The ferroelectric properties of different materials, such as (i) SrTiO₃, oxygen-18 substituted SrTiO₃ and KTaO₃ up to 50 K⁵⁷, (ii) PbZr_{0.5}Ti_{0.5}O₃ thin films up to 4 K⁵⁸, and (iii) antiferroelectric zirconia up to 50 mK⁵⁹, have been characterized for their cryogenic applications.

3.A.2.3. Magnetic Memories

Magnetic random-access memory (MRAM) is another promising resistance-based memory for cryogenic applications, thanks to its high scalability, high speed and low power operation, non-volatility, and compatibility with

Table I: Summary of the Cryogenic Resistance-based Memories.

Type of Memories	Material System	Reported Temperature Range	Effects of Lower Temperature	Performance at Cryogenic Temperatures
RRAM	Pt/Al ₂ O ₃ /HfO _x /Er/Pt ⁴⁸	40 K – 350 K	Larger LRS and HRS	-
	ITO/HfO _x /ITO ⁴⁹	10 K – 490 K	Smaller R _{ON} and Larger R _{OFF}	- Excellent endurance - 5×10^7 cycles - Long retention time - Over 10^6 s.
	Pt/HfO _x /TiN ⁵⁰	4 K and 77 K	Larger HRS and LRS	- Increased SET/RESET voltages at lower T.
	TiN/Ti/HfO ₂ /TiN ⁵¹	4 K – 300 K	No Significant Effect	-
FeRAM	PbZr _{0.5} Ti _{0.5} O ₃ Thin Films ⁵⁸	Up to 4 K	Larger Memory Window	-
	Antiferroelectric Zirconia ⁵⁹	Up to 50 mK	Lower Critical Field (in P-E Curve)	- Endurance – 10^7 cycles
	Si: HfO ₂ based FeFET ⁶⁰	Up to 6.9 K	Larger Memory Window	- Increased program/erase Voltage
MRAM	CoFeB/MgO-based pMTJ ⁶²	Up to 9 K	Higher Magneto-resistance and Larger Switching Voltage	- Better endurance – 10^{12} cycles
	CoFeB-based OST Device ⁶³	Up to 4 K	Low Magneto-resistance	- High speed (~200 ps) - Low error rate (10^{-5})
	Toggle MRAM ⁶⁴	Up to 4.2 K	Enhanced Magneto-resistance	- Improved SNR
QAHE based	tBLG moiré Heterostructure ⁶⁵	Up to 2 K	Enhanced Hall Resistance	- Ultra-low power - Excellent scalability
PCRAM	Perovskite (La, Pr, Ca) MnO ₃ ⁶⁹	Up to 2 K	-	- High distinguish-ability (10^5) between two phases

superconducting cryogenic logic^{25,61}. Magnetic tunnel junction (MTJ), consisting of two ferromagnetic materials (free layer, FL and pinned layer, PL) separated by a thin insulating layer (barrier oxide) [Fig. 4(c)], is the basic building block of MRAMs. For parallel (P) and anti-parallel (AP) magnetization in the two magnetic layers (FL and PL), two levels of magnetoresistance are observed in the MTJ, which are used to define the memory states [see Fig. 4 (g)].

Different magnetic memory devices^{62–64} have been studied at cryogenic conditions to use in cryogenic MRAMs. Lang *et al.*⁶² demonstrated a functioning CoFeB/MgO-based pMTJ device at 9 K temperature that is practical for cryogenic MRAMs. They found a reliable and low error rate ($<10^{-4}$) switching at 9 K. Also, with the lowering of temperature to 9 K, the endurance (over 10^{12} cycles) improves by around three orders. CoFeB based orthogonal spin transfer device has also been studied at 4 K temperature as a cryogenic memory element⁶³. This work has shown high-speed switching (around 200 ps) and a very low error rate (as low as 10^{-5}) which is a significant improvement compared to the room temperature. However, this device achieves this low error rate while writing only within a very limited pulse condition and the read speed is too slow for memory due to their low magnetoresistance. In 2017, Yau *et al.*⁶⁴ characterized a toggle MRAM at 4.2 K for implementing their proposed hybrid JJ-MRAM memory system (discussed in Section 3.C). Along with the successful operation of the toggle MRAM at 4.2 K, this work reported an enhanced magnetoresistance at 4.2 K which improves the signal-to-noise ratio for their proposed hybrid memory system.

3.A.2.4. Other resistance-based Memories

Along with the traditional resistance-based memories, exotic physical (quantum) phenomena can be leveraged to construct cryogenic memories. For example, very recently, a cryogenic non-volatile memory has been proposed based on quantum anomalous Hall effect (QAHE)⁶⁵. QAHE is the precise quantization of Hall resistance at $\pm h/e^2$ (h = Planck's constant, e = charge of an electron) without an external magnetic field. QAHE based memory utilizes these quantized Hall resistance states ($\pm h/e^2$) observed in the twisted bilayer graphene (tBLG) moiré heterostructure⁶⁶ to define the memory states. The schematic of the tBLG heterostructure and the hysteretic behavior of Hall resistance as a function of the bias current are shown in Fig. 4(d) and (h), respectively. This design allows the user to write and read the memory cell by applying nano-ampere level bias currents which eventually makes this design very attractive as an ultra-low-power and highly scalable cryogenic memory.

Phase-change random-access memory (PCRAM) is an emerging non-volatile memory. PCRAMs have been explored for storage applications because of their non-volatility, fast speed, and superb scalability^{67,68}. PCRAMs utilize two phases of chalcogenide materials: the amorphous phase provides high resistance (HRS) and the crystal phase provides low resistance (LRS). A unique hysteretic behavior in resistance as a function of the applied electric field has been observed in (La, Pr, Ca) MnO₃ up to 10 K⁶⁹. These low temperature and stable resistive states can be switched repeatedly with the application of various voltage pulses and hence, the reported behaviors can be utilized for implementing a fast, non-volatile and scalable cryogenic phase-change memory.

Table I summarizes the attempts on cryogenic resistive-based memories along with the effects of cryogenic temperature on their operation and performance.

3.B. Superconducting Memories

Although the non-superconducting memories discussed in Section 3.A can offer excellent scalability, these memories suffer from higher power requirements and lower speed compared to the superconducting SFQ circuits and systems. JJ and SQUID-based SFQ technology has emerged as a promising platform to design the control processor for quantum computers thanks to the requirement of very low operating temperature (4K), high speed, and energy efficiency⁸. Therefore, superconducting memory is an obvious choice for cryogenic applications. However, there is a major drawback: superconductor-insulator-superconductor (SIS) JJ and SQUID-based memories suffer from very low capacity due to the large size memory cells coupled with address lines using transformers which in turn makes the scaling difficult^{70–78}. To circumvent this issue, extensive studies have been carried out on how to improve the capacity of JJ-based cryogenic memory cells. A popular approach to attain high capacity is to pursue the hybrid superconductor-semiconductor schemes combining CMOS technology and Josephson junction-based superconducting technology which we will discuss in the ‘Hybrid Memories’ section. Two feasible alternatives can be the magnetic JJ (MJJ) and superconducting memristor-based memories, which offer high capacity, speed, and energy efficiency while being capable of integration in a single chip with SIS JJs. These traits result in a fast operation, even at a similar clock speed with the fast SFQ control processor and SFQ digital circuits. It is worthwhile to elaborate on superconducting memories in three subsections: (i) SIS JJ-based memories, (ii) magnetic JJ-based memories, and (iii) superconducting memristor-based memories.

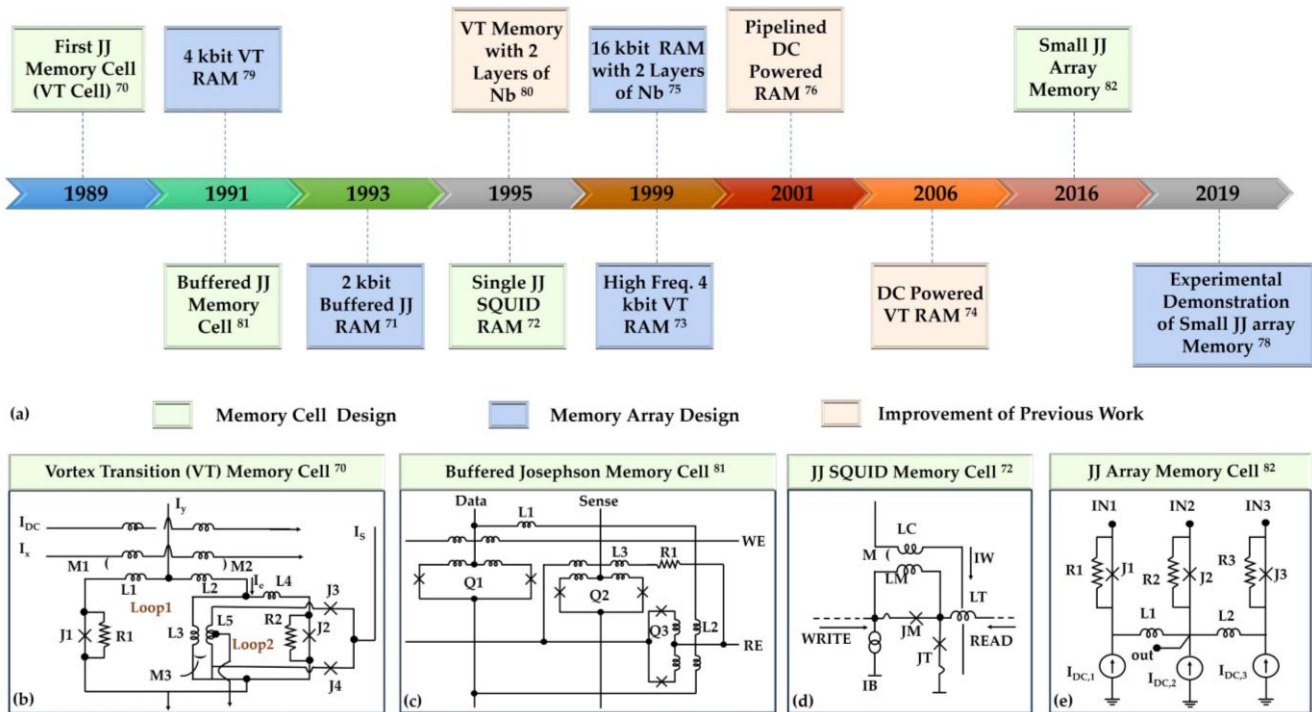


Fig. 5: (a) Timeline demonstrating the enormous research attempts on SIS JJ based memories over the last few decades. Schematics of (b) Josephson vortex transition memory cell ⁷⁰, (c) buffered Josephson memory cell ⁸¹, (d) single JJ SQUID based memory cell ⁷², and (e) three inductively coupled SIS JJs based memory cell ⁸².

3.B.1. SIS JJ-based Memories

SIS JJ-based cryogenic memory design has enjoyed enormous research attention over the last few decades ^{70–78} [summarized in the timeline of Fig. 5 (a)]. Despite all the efforts, these designs suffer from low capacity. To date, only 4 kbit memory has been demonstrated experimentally ⁷³. Tahara *et al.* ⁷⁰ first demonstrated a nondestructive read-out (NDRO) Josephson vortex transition (VT) memory cell in 1989. The memory cell consists of two superconducting loops (contains Nb/AIO_x/Nb JJs and inductors) and a two-junction interferometer gate as a sense gate [schematic shown in Fig. 5(b)]. In Loop 1 and Loop 2, resistors are connected in parallel to JJs (J_1 and J_2) to ensure suitable damping conditions for the junctions. In this design, Loop 1 stores the information in form of an SFQ pulse, and the stored data is read by the switching of the sense gate caused by the vortex transition in Loop 2, which again depends on the stored SFQ pulse in Loop 1. In a later work, two 4-kbit RAMs, composed of 64×64 ⁷⁹ and 256×16 ⁷³ VT memory cells have been demonstrated. Nagasawa *et al.* ⁷⁴ later modified the VT memory cell and proposed a pipeline structure to design a DC-powered RAM. To make this modified VT memory cell able to operate with only DC signals, a two-junction SQUID gate is used as the write gate and a control line is magnetically coupled to Loop 1. In the subsequent work, the VT memory cell was further improved by reducing the number of Nb layers from three to two in fabrication ⁸⁰. Using this improved design, a 16 kbit RAM consisting of four 4 kbit blocks has been demonstrated in Ref. ⁷⁵. A pipelined DC-powered RAM structure has also been proposed later for this 16 kbit Memory ⁷⁶. Yuh *et al.* ⁸¹ demonstrated SQUID-based NDRO memory cell [shown in Fig. 5(c)] which also consists of Nb/AIO_x/Nb JJs and inductors like the VT memory cell and later implemented a 2 kbit RAM using these cells ⁷¹. A major contribution of this design compared to the VT memory cell is that it uses three sense gates instead of one which solves the ‘half select’ problem of SIS JJ-based memories.

In 1995, Polonsky *et al.* ⁷² proposed a new design concept for the JJ-based RAMs shown in Fig. 5(d). The designed memory cell consists of single-junction SQUIDs which are serially connected by the bit lines and coupled inductively to the word lines. Write and read operations are performed by sending pulses in appropriate directions into bit lines and DC pulses with appropriate polarity along word lines.

Recently in 2016, Nair *et al.*^{78,82,83} developed a new design for SIS JJ-based memory cell shown in Fig. 5(e) and experimentally demonstrated the memory operation in 2019. The memory cell consists of three inductively coupled SIS JJs. This design offers three memory states. Write operations are performed by applying SFQ pulses into appropriate junctions and read operation is performed using one of the write mechanisms. Now for example, if the write ‘0’ mechanism is used for the read operation, during the read ‘1’ operation, the memory state will be destructed but read ‘0’ will not be destructive. Therefore, the readout of this memory cell is referred to as half-destructive.

Now, it is worthwhile to discuss and compare the performances of the above-mentioned SIS JJ-based memories. Cell area, speed, memory capacity, and energy efficiency are the major performance metrics for cryogenic memory. Figures 6 (a) and (b) show the cell area, access time, and power consumption for the major attempts on SIS JJ-based memories. Ultra-high-speed and low power consumption of these memories are attractive, but scalability is the major concern for these memories. The table in Fig. 6(c) presents the comparison of the performance of the SIS JJ-based memories.

3.B.2. Magnetic JJ-based Memories

SIS JJ is the main building block of superconducting electronics and the control processor of superconducting qubit-based quantum computers. Therefore, a memory that is compatible with the speed, power, and fabrication method of SIS JJs should be a strong candidate for cryogenic memory applications. However, SIS JJ-based memories suffer from

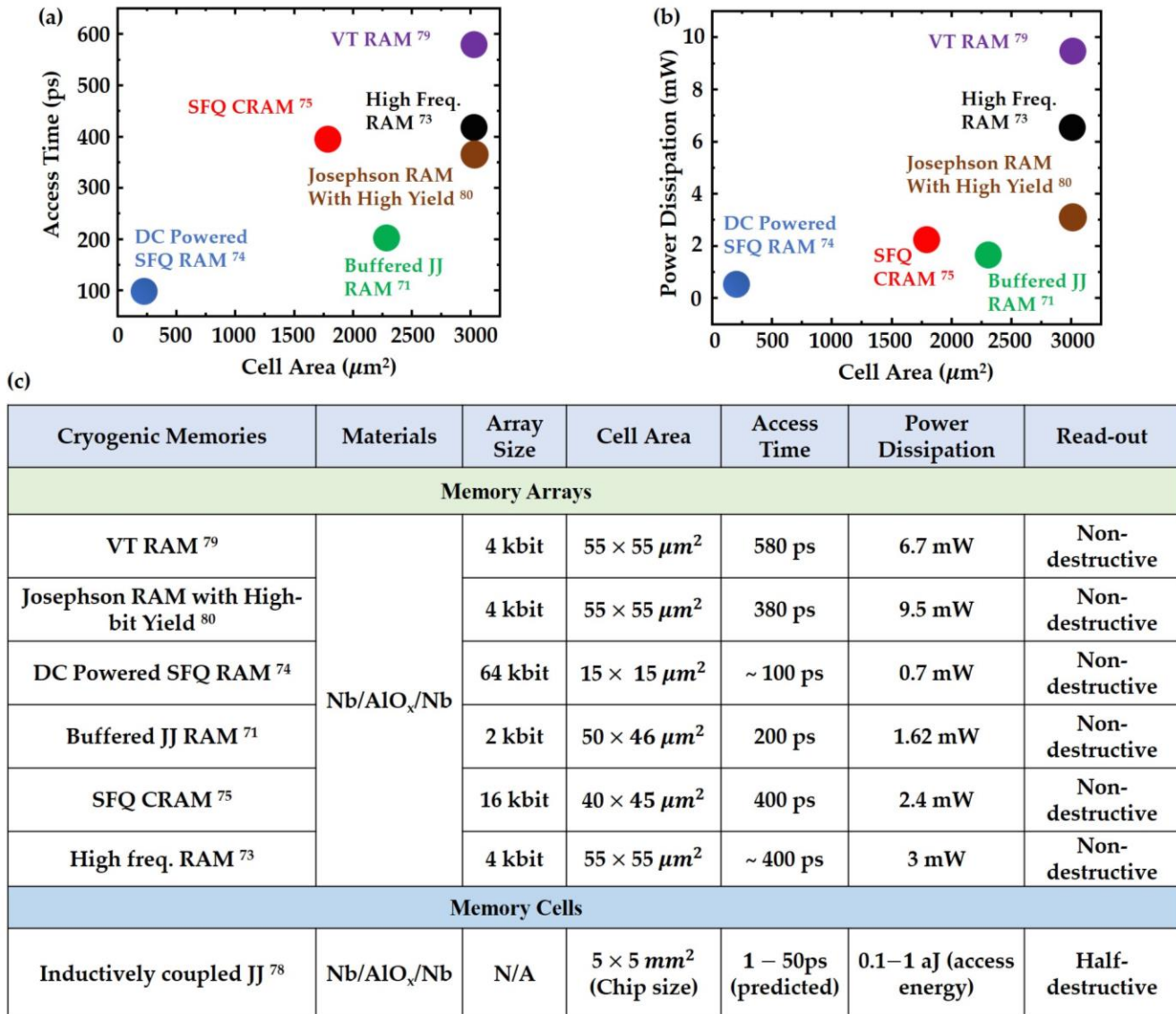


Fig. 6: Comparison of the SIS JJ based memories considering (a) access time and cell area, and (b) power consumption and cell area. (c) A complete comparative study among the major SIS JJ based memories based on some important performance metrics.

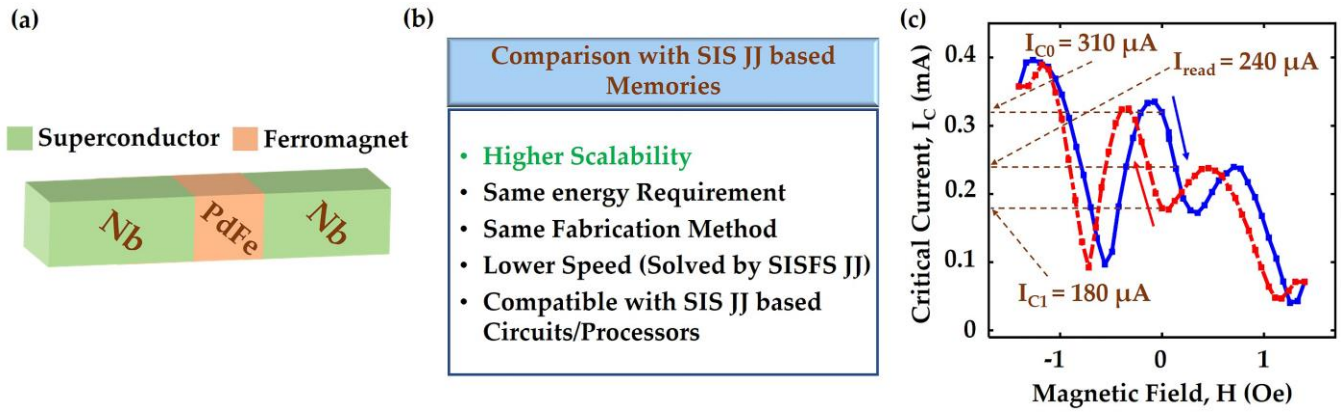


Fig. 7: (a) Schematic of a magnetic JJ structure. (b) Comparison between MJJ and SIS JJ based memories. MJJ offers same speed, requires same power and fabrication method, but can offer more scalability compared to the SIS JJ based memories. (c) Hysteretic dependence of critical current I_C for Nb/Pd_{0.99}Fe_{0.01}/Nb SFS Magnetic Josephson Junction (MJJ) on magnetic field⁸⁵. Magnetic field sweep directions are shown by arrows.

low capacity. As an alternative, in the 1990s⁸⁴, the idea of combining ferromagnetic and superconducting materials to develop a high-capacity cryogenic memory was explored. Magnetic JJ (MJJ) is a version of Josephson junction which is built by sandwiching a ferromagnetic layer between two superconducting materials [schematic shown in Fig. 7(a)]. Figure 7(b) presents a comparison between MJJ-based and SIS JJ-based memories.

MJJ and SIS JJ have the same fabrication process and hence, MJJs can be integrated on a single chip with SIS JJs⁸⁵. The most significant advantage of MJJs is their ability to be in a Josephson state with the inversion of phase difference which is known as π -state^{86,87}. The incorporation of the ferromagnetic layer in the Josephson junction creates a hysteretic dependence of the critical current on the external magnetic field [see Fig. 7(c)]. A small applied magnetic field affects the magnetization of the ferromagnetic layer which eventually changes the I_C of the junction. This change in I_C allows two distinct states to be realized with high (logic '0') and low (logic '1') I_C [marked as I_{C0} and I_{C1} , respectively in Fig. 7(c)]. A small magnetic field, that can be achieved by a small control current, can perform the non-volatile change of I_C of the MJJ based-memories. MJJs are one of the strongest candidates for cryogenic memory in quantum computers and SFQ systems, thanks to their ability of high capacity and compatibility with the SIS JJs.

Ryazanov *et al.*⁸⁵ first proposed the MJJ-based memory with fast and energy-efficient SFQ switching readout. They demonstrated the ability of a superconductor-ferromagnet-superconductor (SFS) JJ (Nb/Pd_{0.99}Fe_{0.01}/Nb) to operate as a Josephson magnetic switch. They utilized the hysteretic behavior of I_C on the external magnetic field in their memory design. The speed of the MJJs depends on the inductance of the control current line and the switching time of SFS junctions. Switching time is given by:

$$\tau_J = \frac{\Phi_0}{2\pi I_C R_N} \quad (1)$$

where Φ_0 is the single flux quantum and R_N is the normal resistance of the junction. SFS JJs show a very small junction characteristic voltage $V_C (= I_C R_N)$ which limits the switching time to ~ 100 ns which is not compatible with the speed of the SIS JJs. To increase V_C , it has been proposed to insert an additional insulator layer with the ferromagnetic material. In the same work, a superconductor-insulator-ferromagnetic-superconductor (SIFS) MJJ (Nb/Al-AlO_x/Pd_{0.99}Fe_{0.01}/Nb) with a higher V_C has been demonstrated retaining the magnetic memory properties. After that, to further increase the speed, the characteristic voltage has been further increased by inserting an additional superconducting layer [SI(S)FS JJ]. Using this SI(S)FS JJ, a maximum V_C of $\sim 400 \mu V$ has been reported that corresponds to a speed of ~ 200 GHz.

Along with the MJJs with one ferromagnetic layer, more than one ferromagnetic layer has been used in MJJs (S/F₁/F₂/.../S). The motivation behind the use of additional ferromagnetic layers is that MJJs with additional ferromagnets allow the ground-state phase difference and critical current of the junction to be tuned by the mutual orientation of the ferromagnetic layers⁸⁸⁻⁹¹. Bell *et al.* first demonstrated spin-valve JJ-based cryogenic memory⁹². A lot of ferromagnetic materials have been later studied in spin-valve JJs which include weak ferromagnetic alloys such as CuNi⁸⁷, PdNi⁹³, and PdFe^{85,94} and strong ferromagnetic elements and alloys such as Ni^{95,96}, Fe⁹⁷, Co⁹⁷, NiFe^{97,98}, NiFeNb⁹⁹, NiFeMo¹⁰⁰, and NiFeCo⁹⁸. Now, let us consider the advantages and disadvantages of using weak and strong ferromagnets in MJJs. Weak ferromagnets have two key advantages over strong ferromagnetic materials. The

first advantage is from the magnetic side which is weak ferromagnets will require less switching energy. Stoner-Wohlfarth theory¹⁰¹ predicts that the switching field required by a single-domain nanomagnet is proportional to the magnetization and also, the switching energy is proportional to the square of its magnetization. Therefore, lower magnetization implies lower switching energy. The second advantage is from the superconducting perspective. Strong ferromagnets have a very short characteristic length scale, ξ_F . ξ_F is the length over which JJs oscillate between 0-junctions and π -junctions with the change in thickness of the ferromagnetic layer. Strong ferromagnetic materials (such as Co or Fe) exhibit ξ_F typically less than 1 nm⁹⁷ which implies that the junction properties will fluctuate even if the average thickness of the ferromagnetic layer changes by a fraction of the atomic monolayer. On the other hand, weak ferromagnets show much larger ξ_F which makes it very easier to control the thickness of the ferromagnets and hence, junction properties show a smaller sample-to-sample variations^{86,98}. In spite of these two strong advantages, weak ferromagnets have not dominated the research on spin-valve JJ based memory due to the severe depression of the critical current being inserted into JJs⁸⁶. The severe depression of the critical current in MJJs will lead to a smaller hysteresis window in the characteristics shown in Fig. 7(c) which will make the sensing of the memory system difficult.

3.B.3. Superconducting Memristor-based Memories

Recent years have witnessed an emergent cryogenic memory technology- a conductance asymmetric SQUID (CA-SQUID). CA SQUID combines the scalability of classical memristors with the ultrafast speed and high energy efficiency of JJs^{102,103}. It utilizes the phase-dependent conductance of JJs and exhibits a pinched hysteresis loop in the current-voltage characteristics reminiscent of the ideal memristors. Figure 8(a) shows the schematic of a CA-SQUID-based superconducting memristor, where two SIS JJs are connected in parallel. Traditionally, the two JJs in CA-SQUID are designed with two different superconducting electrodes to ensure same critical current and asymmetric conductance.

The dynamics of CA-SQUID can be explained with the modified resistively and capacitively shunted junction (RCSJ) model¹⁰⁴⁻¹⁰⁶ with four shunt paths- (i) the Josephson inductance to capture the supercurrent¹⁰⁷, (ii) a constant resistance (R_N) to capture the single-electron tunneling¹⁰⁸, (iii) a capacitance (C_J) due to the junction capacitance, and (iv) a dissipative current path due to the phase-dependent conductance of JJ. Now, with a suitable flux bias ($\Phi = \Phi_0/2$), the effect of critical current can be suppressed while maintaining the asymmetric conductance; it leads to the pinched hysteresis loop in the I - V characteristics of the CA-SQUID [shown in Fig. 8(b)]¹⁰². The two resistance states of the CA-SQUID are used to define the memory states [Fig. 8(c)]. Array level implementations of CA-SQUID is on the horizon. In fact, a recent work¹⁰³ reports a cryogenic memory array design which uses a superconducting memristor-based memory cell and heater cryotron¹⁰⁹-based access device. Superconducting memristors offer distinct advantages, such as high scalability and ultra-fast and energy-efficient operation, which render it a potential candidate for future cryogenic memory applications. Experimental implementation of this novel design concept awaits.

3.C. Hybrid Memories

Conventional non-superconducting memories provide excellent scalability but suffer from lower speed and higher power compared to the JJ-based control processor. On the other hand, SIS JJ-based superconducting memories suffer from very low capacity^{72,73}. To combine the advantages of these two technologies, hybrid memories were proposed. Hybrid technology, which utilizes the best features of each technology, is the potential approach to develop high speed,

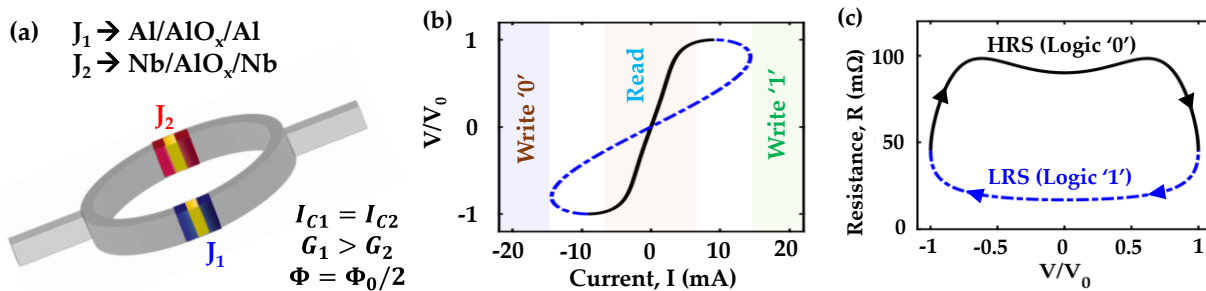


Fig. 8: (a) Schematic of a CA-SQUID device, consisting of two SIS JJs with different superconducting electrodes. Two JJs have the same critical current but different conductance. The application of a magnetic flux of $\Phi_0/2$ suppresses the effect of equal critical current but not the effect of phase-dependent current component, due to the asymmetry in conductance. (b) I - V characteristics and (c) resistance vs voltage characteristics of the CA-SQUID-based superconducting memristor. Two resistance levels [HRS (high resistance state) and LRS (low resistance state)] are utilized to define the memory states. Regions are marked in the I - V characteristics for different memory operations (write and read).

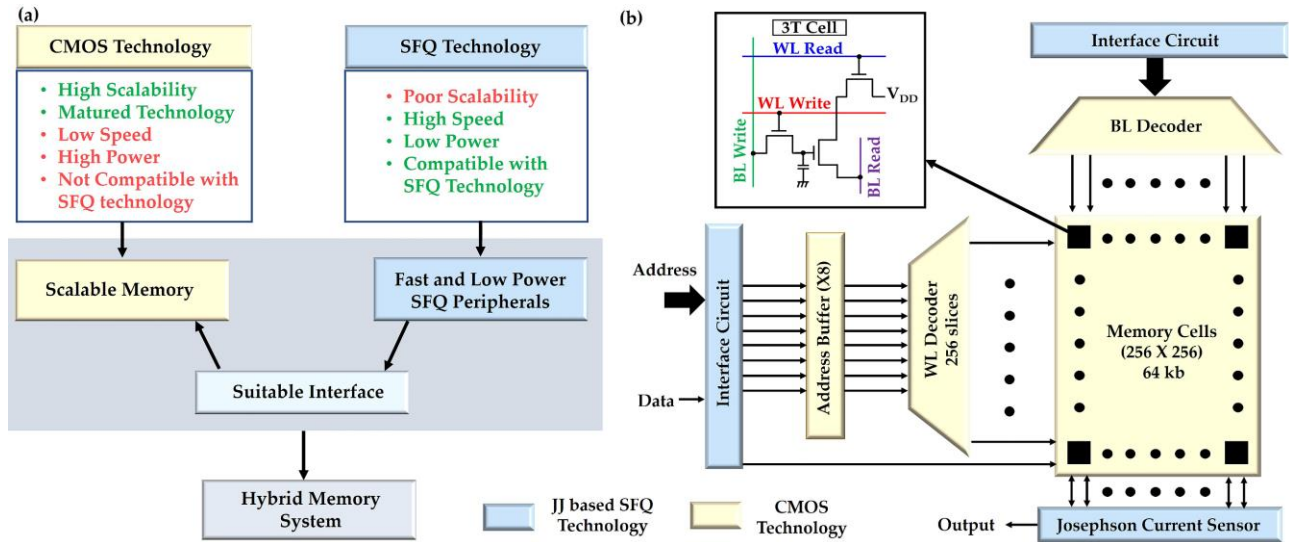


Fig. 9: (a) Illustration of a hybrid memory system, where non-superconducting technology is used as the scalable memory system and superconducting technology is used to access the memory. (b) Example of a hybrid memory system for cryogenic applications proposed in Ref. ¹¹⁰. Here, 3T DRAM is used as the memory element and JJ based circuits are used as the access scheme.

energy-efficient, and high capacity cryogenic memories¹¹⁰. In this approach, highly scalable memories (such as DRAMs, MRAMs, etc.) are used as the storage element, and fast ultra-low-power JJ-based superconductive devices are used to access them. Figure 9(a) illustrates the concept of implementing a hybrid memory system that combines the advantages of both technologies.

Ghoshal *et al.*¹¹⁰ first proposed this approach and some simulations and measurements were reported in their later works^{111–114} to verify the feasibility of the idea. They used 3T DRAMs as the storage element. They demonstrated a 64 kb (256 × 256) hybrid memory system. Figure 9(b) shows the high-level block diagram of their proposed hybrid memory system.

MRAM has also been explored to integrate with Josephson junctions to develop a hybrid cryogenic memory (Josephson-MRAM memory)⁶⁴. This work has first examined the operation of magnetic tunnel junction (MTJ) devices at 4.2 K temperature where a successful switching for MTJ devices has been demonstrated with enhanced magnetoresistance. Spin Hall effect-based MTJ devices have also been explored for cryogenic memory¹¹⁵. In this work, an MTJ patterned on a spin Hall channel is used as a memory cell and a superconductive heater cryotron is used as a control element. This work has demonstrated an energy-efficient (6 pJ per switch switching energy) 4 × 4 array for the designed memory cell. The memory cells in the array can be accessed with 100 μ A current signals which makes the design compatible with SFQ control circuits.

Unlike the two above-mentioned hybrid memories, where two technologies are placed at the same temperature, Mukhanov *et al.*¹¹⁶ suggested a hybrid cryogenic memory system where two technologies were placed at different temperatures. This approach integrates a high-density semiconductor memory at room temperature and a high-speed 4.2 K RSFQ cache that is integrated on a chip with an RSFQ processor. This approach is not suitable for scalable quantum computers due to the interconnection between the room temperature memory and the cryogenic cache, but it is suitable for digital RF receivers due to the high capacity of semiconductor memory and the fast readout ability of superconductive devices. The hybrid memories can be the potential game-changer for the storage system in quantum computing and other cryogenic applications because of their ability to provide a scalable, fast and ultra-low power memory system.

4. Comparative Study of Cryogenic Memories: Pros, Cons, Challenges and Future Prospects

In Section 3, we went over different cryogenic memory technologies. Here we present a comparative study of these technologies in light of the requirements for quantum computing and superconducting electronics applications. The comparative study guides the reader to the advantages, disadvantages offered and challenges faced by these cryogenic memory devices.

The non-superconducting memories such as CMOS DRAMs, resistive, magnetic, and ferroelectric memories are well matured compared to all the other memory technologies. It may take decades for the emerging superconducting

Table II: Comparative Study of the State-of-the-art Cryogenic Memories for Quantum Computers and SFQ Electronics

Comparison Criteria	CMOS DRAM ^{8,10,27}	ReRAM ⁴⁸⁻⁵¹	FeRAM ⁵⁸⁻⁶⁰	MRAM ⁶²⁻⁶⁴	SIS JJ-based ⁷⁰⁻⁸²	Magnetic JJ-based ^{85,92}	Hybrid JJ-CMOS ¹¹⁰⁻¹¹⁴	Hybrid JJ-MRAM ⁶⁴
Maturity of technology for cryogenic applications	Matured for 77 K Uses	In Research	In Research	In Research	Matured	In Research	In Research	In Research
Ideal operating temperature	Above 4 K	Above 4 K	Above 4 K	Above 4 K	4 K/below	4 K/below	4 K	4 K
Can operate at 4 K?	Yes	Yes	Yes	Yes	Yes	Yes	Yes	Yes
Scalable to required capacity?	Yes	Yes	Yes	Yes	No	Yes	Yes	Yes
Compatible with control processor for quantum computers?	No	No	No	No	Yes	Yes	Yes	Yes
Non-volatile?	No	Yes	Yes	Yes	No	No	No	Yes
Cost efficiency	High	High	High	High	Low	Low	Medium	Medium
Thermal leakage	Medium	Medium	Medium	Medium	Very Low	Very Low	Very Low	Very Low
Feasible for very large-scale quantum computers?	No	No	No	No	Yes	Yes	Yes	Yes
Feasible for SFQ circuits?	No	No	No	No	Yes	Yes	Yes	Yes
Existing challenges	Speed, Power & Temp.	Speed, Power & Temp.	Speed, Power & Temp.	Power & Temp.	Poor Scalability	Lack of Suitable Ferro-magnet	Lack of Suitable Interface Circuit	Lack of Suitable Interface Circuit

memories to catch up. Remarkably, all the non-superconducting memories offer significantly better scalability compared to the superconducting memories. However, they face crucial challenges at cryogenic temperatures. In retrospect, most of the conventional memories exhibit successful operation (even with performance improvement in some cases) at a higher temperature (77 K or below), but not at 4 K, implying that these memories are not suitable for integration with the superconducting control processor at 4 K. The memories placed at a higher temperature than 4 K are suitable for the quantum computers with a small number of qubits, but eventually limits the scaling of the quantum computer due to the requirement of interconnects between the control processor and the memory and the resulting thermal leakage of the interconnects. Furthermore, the speed and the power budget of these memories are not compatible with that of the SFQ processors. Some 4 K non-superconducting memories attempt to address this, but they suffer from low-speed and high-power issues compared to the fast and energy-efficient superconducting SFQ circuits, systems, and processors. Therefore, these memories will require a CMOS control processor because these cannot operate at the same speed and the same power budget as the SFQ control processors.

On the other hand, SIS JJ and SQUID-based emerging superconducting memories are very attractive due to their 4 K operations, excellent compatibility with the control processor considering the operating temperature, speed, and power. But the only challenge is the implementation of a high-capacity memory system for quantum computers. To solve this memory array scalability issue, magnetic JJ-based memory and hybrid (cryogenic non-superconducting memories and JJ-based superconducting technology) memories are very attractive. But both of these options suffer from some challenges. Magnetic JJ-based memories offer very suitable compatibility with the SIS JJ-based SFQ circuits/systems/processors in case of integration in the same chip, operating temperature, speed, and power. However, a suitable ferromagnetic material is yet to be found partly because the explored strong and weak ferromagnets suffer from fluctuations resulting from the ferromagnetic layer thickness and the severe depression of the critical current, respectively.

Another alternative for scalable cryogenic memory is the hybrid approach which solves all the issues faced by the non-superconducting memories and the emerging superconducting technology. This approach combines all the best features of both the technologies such as the maturity and high capacity of the non-superconducting memories and the fast and energy-efficient operation of the superconducting circuits. Proper operation at 4 K temperature of the conventional non-superconducting memories has been reported which leaves us with only one challenge to implement this idea which is to find a suitable electrical interface between the non-superconducting and superconducting devices. The interface circuits are mainly cryogenic amplifier circuits used to amplify millivolt signals of Josephson circuits to volt level signals required for CMOS circuits. Superconductor amplifiers¹¹⁷, semiconductor amplifiers¹¹⁸, and hybrid superconductor-semiconductor amplifiers¹¹⁰ have been explored to find suitable Josephson-CMOS interface circuits. The main challenge is that the interface circuit must be chosen in a way so that it can maintain the high-speed, lower power of the whole hybrid system which requires future researches on this field. Note, the hybrid memory utilizing

spin Hall effect-based MTJ and heater cryotron does not suffer from the requirement of an interface circuit like other hybrid memories. We believe, if the scalability issue of the superconducting memories cannot be solved, hybrid memories will be the most feasible and compatible memory device for cryogenic applications.

Table II summarizes the comparative study among the state-of-the-art cryogenic memories which lists the advantages, disadvantages of the cryogenic memories as well as the challenges faced by these memories.

5. Conclusion

Quantum computers and superconducting SFQ circuits/systems are envisioned to replace their conventional counterparts (conventional computers and CMOS electronics, respectively) in near future. However, the lack of a compatible cryogenic memory is one of the major reasons why these two have been limited to only niche applications. In this review, we discussed the major efforts on implementing a suitable cryogenic memory for broader applications. In particular, we highlighted cryogenic characterization of non-superconducting room temperature memories (DRAMs, ReRAMs, MRAMs, FeRAMs, etc.), SIS JJ, and MJJ based superconducting memories, as well as the hybrid memories. We discussed the major challenges faced by these memories in their integration with quantum computers and the SFQ circuits. In brief, cryogenic versions of the non-superconducting memories suffer from speed and power compatibility with the SFQ control processor even though they offer a very high-capacity memory. Conversely, JJ-based emerging memories are compatible with the control processor and SFQ circuits, but they lack scalability owing to their larger size and the requirement of inductive coupling. All points considered, hybrid memories are the most attractive options, because they combine all the advantages of both technologies. However, they lack suitable interface circuits. All these challenges have left the field wide open for future research leveraging novel materials, devices, and architectures.

Data availability

The data that support the plots within this paper are available from the corresponding author on reasonable request.

Author contributions

All authors conceived of this Review. S. A. performed the literature analysis and collected data. All authors took part in writing the manuscript, discussed the data, and contributed to the final manuscript. A. A. supervised the project.

Competing interests

The authors declare no competing interests.

References

1. Mujtaba, H. Cerebras Wafer Scale Engine Is A Massive AI Chip Featuring 2.6 Trillion Transistors & Nearly 1 Million Cores. <https://wccfttech.com/cerebras-unveils-7nm-wafer-scale-engine-2-largest-ai-chip-ever-built/>.
2. Masanet, E., Shehabi, A., Lei, N., Smith, S. & Koomey, J. Recalibrating global data center energy-use estimates. *Science*. **367**, 984–986 (2020) doi:10.1126/science.aba3758.
3. Likharev, K. K. & Lukens, J. Dynamics of Josephson Junctions and Circuits. *Phys. Today* (1988) doi:10.1063/1.2811641.
4. Mukhanov, O. A. *et al.* Superconductor digital-RF receiver systems. *IEICE Trans. Electron.* (2008) doi:10.1093/ietele/e91-c.3.306.
5. Vernik, I. V. *et al.* Cryocooled wideband digital channelizing radio-frequency receiver based on low-pass ADC. in *Superconductor Science and Technology* (2007). doi:10.1088/0953-2048/20/11/S05.
6. NSA. *Superconducting Technology Assessment. National Security Agency Office of Corporate Assessments* (2005).
7. Feynman, R. P. Quantum mechanical computers. *Found. Phys.* (1986) doi:10.1007/BF01886518.
8. Tannu, S. S., Carmean, D. M. & Qureshi, M. K. Cryogenic-DRAM based memory system for scalable quantum computers: A feasibility study. in *ACM International Conference Proceeding Series* (2017). doi:10.1145/3132402.3132436.
9. Filippov, T. V. *et al.* 20 GHz operation of an asynchronous wave-pipelined RSFQ arithmetic-logic unit. in *Physics Procedia* (2012). doi:10.1016/j.phpro.2012.06.130.
10. Ware, F. *et al.* Do superconducting processors really need cryogenic memories? The case for cold DRAM. in *ACM International Conference Proceeding Series* (2017). doi:10.1145/3132402.3132424.
11. Patra, B. *et al.* Cryo-CMOS Circuits and Systems for Quantum Computing Applications. *IEEE J. Solid-State Circuits* (2018) doi:10.1109/JSSC.2017.2737549.
12. Veldhorst, M. *et al.* An addressable quantum dot qubit with fault-tolerant control-fidelity. *Nat. Nanotechnol.* (2014) doi:10.1038/nnano.2014.216.
13. Veldhorst, M. *et al.* A two-qubit logic gate in silicon. *Nature* (2015) doi:10.1038/nature15263.
14. Chow, J. M. *et al.* Implementing a strand of a scalable fault-tolerant quantum computing fabric. *Nat. Commun.* (2014) doi:10.1038/ncomms5015.
15. Dicarlo, L. *et al.* Demonstration of two-qubit algorithms with a superconducting quantum processor. *Nature* (2009) doi:10.1038/nature08121.
16. Kawakami, E. *et al.* Electrical control of a long-lived spin qubit in a Si/SiGe quantum dot. *Nat. Nanotechnol.* (2014) doi:10.1038/nnano.2014.153.
17. Hastings, M. B., Hastings, M. B., Wecker, D., Bauer, B. & Troyer, M. Improving quantum algorithms for quantum chemistry. *Quantum Inf. Comput.* (2014) doi:10.26421/qic15.1-2-1.
18. Shor, P. W. Polynomial-time algorithms for prime factorization and discrete logarithms on a quantum computer. *SIAM J. Comput.* (1997) doi:10.1137/S0097539795293172.
19. Kessler, M. F. The Infrared Space Observatory (ISO) mission. *Adv. Sp. Res.* (2002) doi:10.1016/S0273-1177(02)00557-4.
20. Kirschman, R. K. Low temperature electronic device operation. in *Symp. Electrochemical Society* vol. 14 (1991).
21. Dean, M., Foty, D., Saks, N., Raider, S. & Oleszel, G. Low temperature microelectronics: opportunities and challenges. in *Proc. Symp. Low Temperature Electronic Device Operation, Electrochemical Society* vol. 91 25–37 (1991).
22. Hornibrook, J. M. *et al.* Cryogenic Control Architecture for Large-Scale Quantum Computing. (2015) doi:10.1103/PhysRevApplied.3.024010.
23. Tuckerman, D. B. *et al.* Flexible superconducting Nb transmission lines on thin film polyimide for quantum computing applications. *Supercond. Sci. Technol.* (2016) doi:10.1088/0953-2048/29/8/084007.
24. Likharev, K. K. Superconductor digital electronics. *Phys. C Supercond. its Appl.* (2012) doi:10.1016/j.physc.2012.05.016.
25. Holmes, D. S., Ripple, A. L. & Manheimer, M. A. Energy-Efficient Superconducting Computing—Power Budgets and Requirements. *IEEE Trans. Appl. Supercond.* (2013) doi:10.1109/tasc.2013.2244634.
26. Yoshikawa, N. *et al.* Characterization of 4 K CMOS devices and circuits for hybrid Josephson-CMOS systems. in *IEEE Transactions on Applied Superconductivity* (2005). doi:10.1109/TASC.2005.849786.
27. Henkels, W. H. *et al.* A low temperature 12 ns DRAM. in *International Symposium on VLSI Technology, Systems and Applications* 32–35 (IEEE). doi:10.1109/VTSA.1989.68576.
28. Henkels, W. H. *et al.* Low temperature SER and noise in a high speed DRAM. in *Proceedings of the Workshop on Low Temperature Semiconductor Electronics* (1989) doi:10.1109/ltse.1989.50171.
29. Mohler, R. L. *et al.* A 4-Mb Low-Temperature DRAM. *IEEE J. Solid-State Circuits* **26**, 1519–1529 (1991) doi:10.1109/4.98967.
30. Vogelsang, T. Understanding the energy consumption of Dynamic Random Access Memories. in *Proceedings of the Annual International Symposium on Microarchitecture, MICRO*, 363–374 (2010). doi:10.1109/MICRO.2010.42.
31. Mitchell, C., McCartney, C. L., Hunt, M. & Ho, F. D. Characteristics of a three-transistor DRAM circuit utilizing a ferroelectric transistor. in *Integrated Ferroelectrics* **157**, 31–38, (2014) doi:10.1080/10584587.2014.911620.
32. Tack, M. R., Gao, M., Claeys, C. L. & Declerck, G. J. The Multistable Charge-Controlled Memory Effect in SOI MOS Transistors at Low Temperatures. *IEEE Trans. Electron Devices* (1990) doi:10.1109/16.108200.
33. Morishita, F. *et al.* Leakage mechanism due to floating body and countermeasure on dynamic retention mode of SOI-

- DRAM. in *Symposium on VLSI Technology* (1995). doi:10.1109/vlsit.1995.520897.
34. Ohsawa, T. *et al.* A Memory Using One-transistor Gain Cell on SOI(FBC) with Performance Suitable for Embedded DRAM's. in *IEEE Symposium on VLSI Circuits* (2003). doi:10.1109/vlsic.2003.1221171.
 35. Collaert, N. *et al.* A low-voltage biasing scheme for aggressively scaled bulk FinFET 1T-DRAM featuring 10s retention at 85°C. *Symposium on VLSI Technology* (2010). doi:10.1109/VLSIT.2010.5556211.
 36. Park, K. H., Park, C. M., Kong, S. H. & Lee, J. H. Novel double-gate 1T-DRAM cell using nonvolatile memory functionality for high-performance and highly scalable embedded DRAMs. *IEEE Trans. Electron Devices* (2010) doi:10.1109/TED.2009.2038650.
 37. Bae, J. H. *et al.* Characterization of a Capacitorless DRAM Cell for Cryogenic Memory Applications. *IEEE Electron Device Lett.* (2019) doi:10.1109/LED.2019.2933504.
 38. Song, Y. J., Jeong, G., Baek, I. G. & Choi, J. What lies ahead for resistance-based memory technologies? *Computer (Long Beach, Calif.)* **46**, 30–36 (2013) doi:10.1109/MC.2013.221.
 39. Govoreanu, B. *et al.* 10×10nm² Hf/HfO_x crossbar resistive RAM with excellent performance, reliability and low-energy operation. in *International Electron Devices Meeting, IEDM* (2011). doi:10.1109/IEDM.2011.6131652.
 40. Lee, H. Y. *et al.* Evidence and solution of over-RESET problem for HfOX based resistive memory with sub-ns switching speed and high endurance. in *International Electron Devices Meeting, IEDM* (2010). doi:10.1109/IEDM.2010.5703395.
 41. Ielmini, D. *et al.* Scaling analysis of submicrometer nickel-oxide-based resistive switching memory devices. *J. Appl. Phys.* (2011) doi:10.1063/1.3544499.
 42. Kügeler, C., Zhang, J., Hoffmann-Eifert, S., Kim, S. K. & Waser, R. Nanostructured resistive memory cells based on 8-nm-thin TiO₂ films deposited by atomic layer deposition. *J. Vac. Sci. Technol. B* (2011) doi:10.1116/1.3536487.
 43. Walczyk, C. *et al.* On the role of Ti adlayers for resistive switching in HfO₂-based metal-insulator-metal structures: Top versus bottom electrode integration. *J. Vac. Sci. Technol. B* (2011) doi:10.1116/1.3536524.
 44. Hirose, S., Nakayama, A., Niimi, H., Kageyama, K. & Takagi, H. Resistance switching and retention behaviors in polycrystalline La-doped SrTiO₃ ceramics chip devices. *J. Appl. Phys.* (2008) doi:10.1063/1.2975316.
 45. Yao, J., Sun, Z., Zhong, L., Natelson, D. & Tour, J. M. Resistive switches and memories from silicon oxide. *Nano Lett.* (2010) doi:10.1021/nl102255r.
 46. Lörtscher, E., Cizek, J. W., Tour, J. & Riel, H. Reversible and controllable switching of a single-molecule junction. *Small* (2006) doi:10.1002/sml.200600101.
 47. Walczyk, C. *et al.* Impact of temperature on the resistive switching behavior of embedded HfO₂-based RRAM devices. *IEEE Trans. Electron Devices* (2011) doi:10.1109/TED.2011.2160265.
 48. Ahn, C. *et al.* Temperature-dependent studies of the electrical properties and the conduction mechanism of HfO_x-based RRAM. in *International Symposium on VLSI Technology, Systems and Application, VLSI-TSA 2014* (2014). doi:10.1109/VLSI-TSA.2014.6839685.
 49. Shang, J. *et al.* Thermally stable transparent resistive random access memory based on all-oxide heterostructures. *Adv. Funct. Mater.* (2014) doi:10.1002/adfm.201303274.
 50. Fang, R., Chen, W., Gao, L., Yu, W. & Yu, S. Low-temperature characteristics of HfO. *IEEE Electron Device Lett.* **36**, 567–569 (2015).
 51. Blonkowski, S. & Cabout, T. Bipolar resistive switching from liquid helium to room temperature. *J. Phys. D: Appl. Phys.* (2015) doi:10.1088/0022-3727/48/34/345101.
 52. Scott, J. F. & Paz De Araujo, C. A. Ferroelectric memories. *Science*. (1989) doi:10.1126/science.246.4936.1400.
 53. Trentzsch, M. *et al.* A 28nm HKMG super low power embedded NVM technology based on ferroelectric FETs. in *International Electron Devices Meeting, IEDM* (2017). doi:10.1109/IEDM.2016.7838397.
 54. Dünkler, S. *et al.* A FeFET based super-low-power ultra-fast embedded NVM technology for 22nm FDSOI and beyond. in *International Electron Devices Meeting, IEDM* (2018). doi:10.1109/IEDM.2017.8268425.
 55. Chatterjee, K. *et al.* Self-Aligned, Gate Last, FDSOI, Ferroelectric Gate Memory Device with 5.5-nm Hf_{0.8}Zr_{0.2}O₂, High Endurance and Breakdown Recovery. *IEEE Electron Device Lett.* (2017) doi:10.1109/LED.2017.2748992.
 56. Florent, K. *et al.* Vertical Ferroelectric HfO₂ FET based on 3-D NAND Architecture: Towards Dense Low-Power Memory. in *International Electron Devices Meeting, IEDM* (2019). doi:10.1109/IEDM.2018.8614710.
 57. Rowley, S. E. *et al.* Ferroelectric quantum criticality. *Nat. Phys.* (2014) doi:10.1038/nphys2924.
 58. Meng, X. J. *et al.* Temperature dependence of ferroelectric and dielectric properties of PbZr_{0.5}Ti_{0.5}O₃ thin film based capacitors. *Appl. Phys. Lett.* **81**, 4035–4037 (2002) doi:10.1063/1.1522833.
 59. Wang, Z. *et al.* Cryogenic Characterization of Antiferroelectric Zirconia down to 50 mK. in *Device Research Conference, DRC* (2019). doi:10.1109/DRC46940.2019.9046475.
 60. Wang, Z. *et al.* Cryogenic characterization of a ferroelectric field-effect-transistor. *Appl. Phys. Lett.* (2020) doi:10.1063/1.5129692.
 61. Rehm, L. *et al.* Sub-nanosecond switching in a cryogenic spin-torque spin-valve memory element with a dilute permalloy free layer. *Appl. Phys. Lett.* **114**, 212402 (2019) doi:10.1063/1.5094924.
 62. Lang, L. *et al.* A low temperature functioning CoFeB/MgO-based perpendicular magnetic tunnel junction for cryogenic nonvolatile random access memory. *Appl. Phys. Lett.* **116**, (2020) doi:10.1063/1.5129553.
 63. Rowlands, G. E. *et al.* A cryogenic spin-torque memory element with precessional magnetization dynamics. *Sci. Rep.*

- (2019) doi:10.1038/s41598-018-37204-3.
64. Yau, J. B., Fung, Y. K. K. & Gibson, G. W. Hybrid cryogenic memory cells for superconducting computing applications. in *2017 IEEE International Conference on Rebooting Computing, ICRC 2017 - Proceedings* (2017). doi:10.1109/ICRC.2017.8123684.
 65. Alam, S., Hossain, M. S. & Aziz, A. A non-volatile cryogenic random-access memory based on the quantum anomalous Hall effect. *Sci. Rep.* **11**, 1–9 (2021) doi:10.1038/s41598-021-87056-7.
 66. Serlin, M. *et al.* Intrinsic quantized anomalous Hall effect in a moiré heterostructure. *Science*. **367**, 900–903 (2020) doi:10.1126/science.aay5533.
 67. Ovshinsky, S. R. Reversible electrical switching phenomena in disordered structures. *Phys. Rev. Lett.* **21**, 1450–1453 (1968) doi:10.1103/PhysRevLett.21.1450.
 68. Lai, S. Current status of the phase change memory and its future. in *International Electron Devices Meeting 255–258* (2003). doi:10.1109/iedm.2003.1269271.
 69. Yi, H. T., Choi, T. & Cheong, S. W. Reversible colossal resistance switching in (La,Pr,Ca) MnO₃: Cryogenic nonvolatile memories. *Appl. Phys. Lett.* (2009) doi:10.1063/1.3204690.
 70. Tahara, S., Ishida, I., Ajisawa, Y. & Wada, Y. Experimental vortex transitional nondestructive read-out Josephson memory cell. *J. Appl. Phys.* (1989) doi:10.1063/1.343077.
 71. Yuh, P. F. A 2-kbit Superconducting Memory Chip. *IEEE Trans. Appl. Supercond.* **3**, 3013–3021 (1993) doi:10.1109/77.257228.
 72. Polonsky, S. V., Kirichenko, A. F., Semenov, V. K. & Likharev, K. K. Rapid Single Flux Quantum Random Access Memory. *IEEE Trans. Appl. Supercond.* (1995) doi:10.1109/77.403223.
 73. Nagasawa, S., Numata, H., Hashimoto, Y. & Tahara, S. High-frequency clock operation of Josephson 256-word x 16-bit rams. *IEEE Trans. Appl. Supercond.* (1999) doi:10.1109/77.783834.
 74. Nagasawa, S., Hinode, K., Satoh, T., Kitagawa, Y. & Hidaka, M. Design of all-dc-powered high-speed single flux quantum random access memory based on a pipeline structure for memory cell arrays. *Supercond. Sci. Technol.* (2006) doi:10.1088/0953-2048/19/5/S34.
 75. Kirichenko, A., Mukhanov, O., Kirichenko, A. F., Mukhanov, O. A. & Brock, D. K. A Single Flux Quantum Cryogenic Random Access Memory. in *Extended Abstracts of 7th International Superconducting Electronics Conference (ISEC'99)* 124–127 (1999).
 76. Kirichenko, A. F., Sarwana, S., Brock, D. K. & Radpavar, M. Pipelined DC-powered SFQ RAM. in *IEEE Transactions on Applied Superconductivity* (2001). doi:10.1109/77.919401.
 77. Alam, S., Jahangir, M. A. & Aziz, A. A Compact Model for Superconductor- Insulator-Superconductor (SIS) Josephson Junctions. *IEEE Electron Device Lett.* **41**, 1249–1252 (2020). doi: 10.1109/LED.2020.3002448.
 78. Nair, N., Jafari-Salim, A., D'Addario, A., Imam, N. & Braiman, Y. Experimental demonstration of a Josephson cryogenic memory cell based on coupled Josephson junction arrays. *Supercond. Sci. Technol.* **32**, 115012 (2019) doi:10.1088/1361-6668/ab416a.
 79. Tahara, S. *et al.* 4-Kbit Josephson Nondestructive ReadOut Ram Operated At 580 psec and 6.7 mW. *IEEE Trans. Magn.* (1991) doi:10.1109/20.133751.
 80. Nagasawa, S., Hashimoto, Y., Numata, H. & Tahara, S. A 380 ps, 9.5 mW Josephson 4-Kbit RAM Operated at a High Bit Yield. *IEEE Trans. Appl. Supercond.* (1995) doi:10.1109/77.403086.
 81. Yuh, P. F. A Buffered Nondestructive-Readout Josephson Memory Cell with Three Gates. *IEEE Trans. Magn.* (1991) doi:10.1109/20.133809.
 82. Braiman, Y., Neschke, B., Nair, N., Imam, N. & Glowinski, R. Memory states in small arrays of Josephson junctions. *Phys. Rev. E* (2016) doi:10.1103/PhysRevE.94.052223.
 83. Nair, N. & Braiman, Y. A ternary memory cell using small Josephson junction arrays. *Supercond. Sci. Technol.* (2018) doi:10.1088/1361-6668/aae2a9.
 84. Hidaka, Y. Superconductor magnetic memory using magnetic films. U.S. Patent No. 5,039,656 (1991).
 85. Ryazanov, V. V. *et al.* Magnetic Josephson junction technology for digital and memory applications. in *Physics Procedia* (2012). doi:10.1016/j.phpro.2012.06.126.
 86. Oboznov, V. A., Bol'ginov, V. V., Feofanov, A. K., Ryazanov, V. V. & Buzdin, A. I. Thickness dependence of the Josephson ground states of superconductor-ferromagnet-superconductor junctions. *Phys. Rev. Lett.* (2006) doi:10.1103/PhysRevLett.96.197003.
 87. Ryazanov, V. V. *et al.* Coupling of two superconductors through a ferromagnet: Evidence for a π junction. *Phys. Rev. Lett.* (2001) doi:10.1103/PhysRevLett.86.2427.
 88. Bergeret, F. S., Volkov, A. F. & Efetov, K. B. Enhancement of the Josephson current by an exchange field in superconductor-ferromagnet structures. *Phys. Rev. Lett.* (2001) doi:10.1103/PhysRevLett.86.3140.
 89. Krivoruchko, V. N. & Koshina, E. A. From inversion to enhancement of the dc Josephson current in (formula presented) tunnel structures. *Phys. Rev. B - Condens. Matter Mater. Phys.* (2001) doi:10.1103/PhysRevB.64.172511.
 90. Golubov, A. A., Kupriyanov, M. Y. & Fominov, Y. V. Critical current in SFIFS junctions. *JETP Lett.* (2002) doi:10.1134/1.1475721.
 91. Barash, Y. S., Bobkova, I. V. & Kopp, T. Josephson current in S-FIF-S junctions: Nonmonotonic dependence on

- misorientation angle. *Phys. Rev. B - Condens. Matter Mater. Phys.* (2002) doi:10.1103/PhysRevB.66.140503.
92. Bell, C. *et al.* Controllable Josephson current through a pseudospin-valve structure. *Appl. Phys. Lett.* **84**, 1153–1155 (2004) doi:10.1063/1.1646217.
 93. Kontos, T. *et al.* Josephson Junction through a Thin Ferromagnetic Layer: Negative Coupling. *Phys. Rev. Lett.* (2002) doi:10.1103/PhysRevLett.89.137007.
 94. Glick, J. A., Loloee, R., Pratt, W. P. & Birge, N. O. Critical Current Oscillations of Josephson Junctions Containing PdFe Nanomagnets. *IEEE Trans. Appl. Supercond.* (2017) doi:10.1109/TASC.2016.2630024.
 95. Blum, Y., Tsukernik, A., Karpovski, M. & Palevski, A. Oscillations of the Superconducting Critical Current in Nb-Cu-Ni-Cu-Nb Junctions. *Phys. Rev. Lett.* (2002) doi:10.1103/PhysRevLett.89.187004.
 96. Shelukhin, V. *et al.* Observation of periodic π -phase shifts in ferromagnet-superconductor multilayers. *Phys. Rev. B - Condens. Matter Mater. Phys.* (2006) doi:10.1103/PhysRevB.73.174506.
 97. Robinson, J. W. A., Piano, S., Burnell, G., Bell, C. & Blamire, M. G. Critical current oscillations in strong ferromagnetic π junctions. *Phys. Rev. Lett.* (2006) doi:10.1103/PhysRevLett.97.177003.
 98. Glick, J. A. *et al.* Critical current oscillations of elliptical Josephson junctions with single-domain ferromagnetic layers. *J. Appl. Phys.* (2017) doi:10.1063/1.4989392.
 99. Baek, B., Rippard, W. H., Benz, S. P., Russek, S. E. & Dresselhaus, P. D. Hybrid superconducting-magnetic memory device using competing order parameters. *Nat. Commun.* (2014) doi:10.1038/ncomms4888.
 100. Niedzielski, B. M., Gingrich, E. C., Loloee, R., Pratt, W. P. & Birge, N. O. S/F/S Josephson junctions with single-domain ferromagnets for memory applications. *Supercond. Sci. Technol.* (2015) doi:10.1088/0953-2048/28/8/085012.
 101. Stoner, E. C. & Wohlfarth, E. P. A mechanism of magnetic hysteresis in heterogeneous alloys. *IEEE Trans. Magn.* (1991) doi:10.1109/TMAG.1991.1183750.
 102. Peotta, S. & Di Ventra, M. Superconducting Memristors. *Phys. Rev. Appl.* (2014) doi:10.1103/PhysRevApplied.2.034011.
 103. Alam, S., Hossain, M. S. & Aziz, A. A cryogenic memory array based on superconducting memristors. *Appl. Phys. Lett.* **119**, 082602 (2021).
 104. Stewart, W. C. Current-voltage characteristics of Josephson junctions. *Appl. Phys. Lett.* (1968) doi:10.1063/1.1651991.
 105. McCumber, D. E. Effect of ac impedance on dc voltage-current characteristics of superconductor weak-link junctions. *J. Appl. Phys.* (1968) doi:10.1063/1.1656743.
 106. Alam, S., Jahangir, M. A. & Aziz, A. A Compact Model for Superconductor- Insulator-Superconductor (SIS) Josephson Junctions. *IEEE Electron Device Lett.* **41**, 1249–1252 (2020).
 107. Ingold, G. L., Grabert, H. & Eberhardt, U. Cooper-pair current through ultrasmall Josephson junctions. *Phys. Rev. B* (1994) doi:10.1103/PhysRevB.50.395.
 108. Van Den Brink, A. M., Schön, G. & Geerligs, L. J. Combined single-electron and coherent-Cooper-pair tunneling in voltage-biased Josephson junctions. *Phys. Rev. Lett.* (1991) doi:10.1103/PhysRevLett.67.3030.
 109. McCaughan, A. N. & Berggren, K. K. A superconducting-nanowire three-terminal electrothermal device. *Nano Lett.* (2014) doi:10.1021/nl502629x.
 110. Ghoshal, U., Kroger, H. & Van Duzer, T. Superconductor-Semiconductor Memories. *IEEE Transactions on Applied Superconductivity* (1993) doi:10.1109/77.233542.
 111. Feng, Y. J. *et al.* Josephson-CMOS hybrid memory with ultra-high-speed interface circuit. in *IEEE Transactions on Applied Superconductivity* (2003). doi:10.1109/TASC.2003.813902.
 112. Duzer, T. Van, Liu, Q., Meng, X., Whiteley, S. & Yoshikawa, N. High-speed interface amplifiers for SFQ-to-CMOS signal conversion. in *International Superconductor Electronics Conference, ISEC* (2003).
 113. Liu, Q. *et al.* Simulation and measurements on a 64-kbit hybrid Josephson-CMOS memory. in *IEEE Transactions on Applied Superconductivity* (2005). doi:10.1109/TASC.2005.849863.
 114. Liu, Q. *et al.* Latency and power measurements on a 64-kb hybrid Josephson-CMOS memory. in *IEEE Transactions on Applied Superconductivity* (2007). doi:10.1109/TASC.2007.898698.
 115. Nguyen, M. H. *et al.* Cryogenic Memory Architecture Integrating Spin Hall Effect based Magnetic Memory and Superconductive Cryotron Devices. *Sci. Rep.* (2020) doi:10.1038/s41598-019-57137-9.
 116. Mukhanov, O. A., Kirichenko, A. F., Filippov, T. V. & Sarwana, S. Hybrid semiconductor-superconductor fast-readout memory for digital RF receivers. in *IEEE Transactions on Applied Superconductivity* (2011). doi:10.1109/TASC.2010.2089409.
 117. Suzuki, H., Inoue, A., Imamura, T. & Hasuo, S. Josephson driver to interface Josephson junctions to semiconductor transistors. in *International Electron Devices Meeting* 290–293 (Publ by IEEE, 1988). doi:10.1109/iedm.1988.32814.
 118. Ghoshal, U., Kishore, S., Feldman, A., Huynh, L. & Van Duzer, T. CMOS amplifier designs for Josephson-CMOS interface circuits. *IEEE Trans. Appl. Supercond.* **5**, 2640–2643 (1995) doi:10.1109/77.403132.